Polymer Chemistry

Property Impact of Common Linker Segments in Sequence-Controlled Polyesters

Journal:	*Polymer Chemistry*
Manuscript ID	PY-ART-10-2018-001443.R1
Article Type:	Paper
Date Submitted by the Author:	09-Nov-2018
Complete List of Authors:	Swisher, Jordan H; University of Pittsburgh, Chemistry Nowalk, Jamie A; University of Pittsburgh, Chemistry Meyer, Tara; University of Pittsburgh, Department of Chemistry

Journal Name

ARTICLE

Property Impact of Common Linker Segments in Sequence-Controlled Polyesters

Jordan H. Swisher[a], Jamie A. Nowalk[a], and Tara Y. Meyer *[,a,b]

Received 00th January 20xx,
Accepted 00th January 20xx

DOI: 10.1039/x0xx00000x

www.rsc.org/

Heterogeneous "linkers" are incorporated into polymers for a number of reasons, most commonly to facilitate the coupling of the targeted backbone segments. Due to their inclusion in the backbone, these linkers have the potential to affect the overall properties of the copolymer, even when present in relatively low weight percentages. To characterize the degree of impact of some common linkers, a set of polymers that incorporate both degradable sequenced segments and linkers were synthesized and systematically examined. Seven sequence-controlled olefin containing ester macrocycles were prepared, each with a unique central moiety, including a five-carbon alkyl chain, diethylene glycol, a urea, a thioether, a triazole, a bioaromatic, and an extension of the ester sequence. The macrocycles were polymerized via ED-ROMP to yield seven polymers that vary only in the the linker segment. The properties of all polymers were compared to determine the relative dominance of the different linker types. The properties tested in the study included thermal behavior, mechanical characteristics, hydrolytic degradation and film qualities. The thermal and mechanical properties proved to be dependent primarily on the ability of the linker to promote interchain interactions, as well as the weight fraction of the linker, whereas the hydrolytic degradation was dominated by the relative hydrophobicity of the linker groups. In all cases, the linker identity was a significant contributer to the behavior.

Introduction

The preparation and investigation of sequence-controlled polymers (SCPs) is a rapidly growing area of macromolecular research, and the importance of SCPs is ever rising as their unique and desirable properties are discovered.(1) Sequence-control in polymers has been used for information storage,(2-9) precise folding and self-assembly,(10-17) molecular recognition, enhanced photophysical properties,(18-24) and more.(25) In recent studies, for example, we have shown that sequence matters in the hydrolytic degradation of biodegradable polyesters, such as poly(lactic-*co*-glycolic acid) (PLGA).(26-31) By controlling monomer order, the degradation behaviors were enhanced when compared to random analogues, allowing tunability of degradation rates based upon sequence in addition to composition and molecular weight. The challenge that remains in the field of SCPs is synthetic accessibility and scalability.

When preparing SCPs, it is often necessary to include additional components that are not structurally homogenous with the monomers. Groups such as click-chemistry linkers,(32-35) step-growth polymerization functional handles,(36) polymerization triggers,(37) and other moieties,(38, 39) are often incorporated into the backbone of SCPs. Each of these moieties serve an important role in the preparation of these materials, but when moving toward applications or desired properties, it is important to determine the effect of these backbone segments on the overall behavior of the polymer.

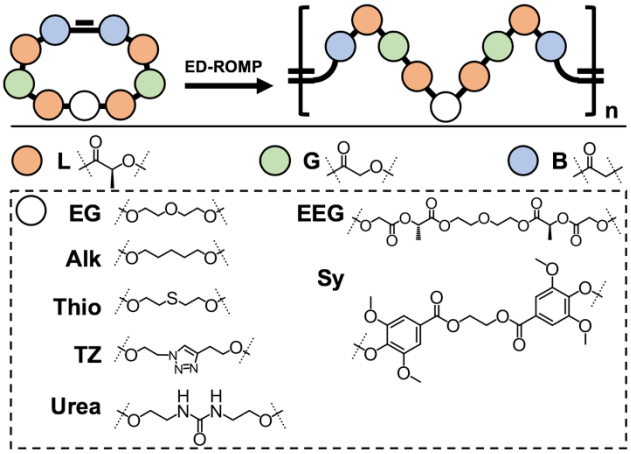

Figure 1. Representation of sequence-controlled polymer with variable linker unit.

Our interest in this study arose from our prior observation of a linker effect in sequenced polyesters that we assembled using entropy-driven ring-opening polymerization (ED-ROMP).(28) Macrocyclic monomers, containing both an ethylene glycol and an α,ω-dialkene linker, were polymerized using ED-ROMP to create polymers incorporating the targeted polyester sequence with molecular weight control. Despite the successes of using ED-ROMP as a general and scalable method

[a] *Department of Chemistry, University of Pittsburgh, Pittsburgh, Pennsylvania 15260, United States.*
[b] *McGowan Center for Regenerative Medicine, University of Pittsburgh, Pittsburgh, Pennsylvania 15260, United States.*
** Corresponding author, tmeyer@pitt.edu*
Electronic Supplementary Information (ESI) available: [details of any supplementary information available should be included here]. See DOI: 10.1039/x0xx00000x

to prepare SCPs, the incorporation of two conformationally-flexible linkers resulted in a glass transition temperature (T_g) well below that required for bioengineering applications. This study inspired us to investigate how other common linker segments that could potentially be used in our materials would impact the properties of these polyesters and to determine, in particular, whether these linkers would affect the targeted sequence-related degradation (Figure 1).

To quantify the impact of linker structure on mechanical, thermal, and degradation properties, a set of polymers with identical sequence and monomer composition and a variable central linker were prepared via ED-ROMP. In this case, we replaced the ethylene glycol linker from our previous study with a series of alternatives. We chose to study this polyester system because of the high sequence-fidelity associated with ED-ROMP of ester macrocycles, along with our understanding of the synthesis and behavior of related polymers. The linkers in this study include a C5 carbon chain, an ethylene glycol, a urea, an aromatic ester, thioether, triazole, as well as an extension of the ester sequence (additional lactic and glycolic acid). In so doing, we have not only demonstrated the power of the ED-ROMP strategy to create sequenced copolymers that incorporate a range of additional functionality but also investigated the impacts these functional groups have on the properties of the prepared polymers. Herein, we describe the results of this study and discuss their relevance to this approach to preparing SCPs.

Experimental

Materials

All chemicals were purchased and used without purification unless specified otherwise. See supplementary information for further details.

Synthesis

See supplementary information for detailed synthesis and characterization information.

Methods

NMR (^{1}H and ^{13}C) NMR spectra were acquired in $CDCl_3$, MeOD or d-DMSO (Cambridge Isotope Laboratories, Inc.) using Bruker spectrometers (400, 500 MHz) and calibrated to residual solvent peaks (δ7.26 and δ77.13 for $CDCl_3$, δ3.31 and δ49.00 for MeOD, and δ2.50 and δ39.52 for d-DMSO). See supporting information for all NMR spectra.

Size-exclusion chromatography (SEC) was carried out using a TOSOH HLC-8320GPC EcoSEC equipped with two columns (TSK-3000H, TSK-4000H). A mobile phase of THF inhibited with 0.025% butylated hydroxytoluene (Fisher Scientific, Inc.) at 40 °C was used with a set of polystyrene standards (2.5, 9, 30, 50 and 92 kDa) (Sigma-Aldrich, Inc.) to determine reported M_n, M_W and Đ data.

Inductively-Coupled Plasma – Optical Emission Spectroscopy (ICP-OES) analysis was performed using an argon flow with a Perkin Elmer Optima spectrometer. A 5% v/v nitric acid matrix was prepared by diluting nitric acid (Sigma Aldrich, > 99.999% trace metal basis) with NANOpure® (Thermo Scientific, > 18.2 MΩ · cm) water, and all samples were digested in concentrated nitric acid. Unknown Ru concentrations were determined by comparison to a 7-point standard curve with a range of 0.10 - 10 ppm Ru (0.10, 0.50, 1.0, 2.5, 5.0, 7.5, and 10 ppm Ru prepared by volume), prepared using a ruthenium standard for ICP (Inorganic Ventures, 1003 ± 5 μg/mL Ru in 10% HCl) diluted in a 5% nitric acid matrix. All standards and unknown samples were measured 6 times and averaged. A 7 min flush time with 5% nitric acid matrix was used between all runs, and a blank was analyzed before each unknown sample to confirm removal of all residual metals from the instrument.

Differential scanning calorimetry (DSC) was performed with a TA Instruments Q200 DSC. Standard data were collected with a heating and cooling rate of 10 °C/min under nitrogen flow (20 mL/min) with two heating and cooling cycles from -10 °C – 200 °C. Degraded polymer sample data was collected with only one heating and cooling cycle.

Thermogravimetric analysis (TGA) was performed with a TA Instruments Q500 TGA. Standard data were collected by heating from RT to 500 °C with a heating rate of 10°C/min.

Pd sputter coating was performed using a Cressington sputter coater. The coater was flushed with argon and evacuated three times and then samples were coated for 60 seconds.

Scanning electron microscopy (SEM) was performed on Pd-coated samples using a JEOL JSM 6610 Low-Vac SEM. Images were taken using secondary electron imaging (SEI) with an acceleration voltage of 5 kV under high vacuum.

Optical profilometry was performed using a Bruker Contour Elite I optical profilometer. Samples were sliced to create a step indicative of film thickness, and sputter coated with Pd to give uniform reflectiveness, and then analyzed. (See supporting information for optical profiles, Figure S1-7)

Nanoindentation was performed using a Hysitron TI 950 Triboindenter with a Berkovich diamond indenter tip. See supporting information and Figure S8 for methods and for data analysis.

Film Degradation Study

Films were prepared by casting 18 μL of a 100 mg/mL chloroform solution of each polymer onto pre-weighed 7 mm aluminum foil discs. Resulting films weighed 1.5 - 2.1 mg on average and ranged from 15-35 μm in thickness. Films were then air dried for 24 h in a fume hood and then dried in vacuo for 72 h. The films were placed into individual pre-weighed vials along with 3 mL of PBS buffer. Vials were then shaken lightly at 37°C until removal. Upon removal, films were rinsed three times with DI water, flash frozen with liquid nitrogen and lyophilized for at least 2 h. Film appearance, mass and molecular weight were monitored with time, and samples were also taken for DSC and SEM as the M_n of the polymer approached 50% of its original value. At least three films were used for each reported data point before day 70, and associated error bars represent the standard deviation in both the positive and negative direction. On and after day 70, at least 2 films were used for

reach reported data point, and associated error bars represent the range in both the positive and negative direction.

Results and Discussion

Polymer Synthesis

Olefin containing macrocycles were prepared via orthogonal protection, deprotection and ester coupling strategies (Scheme 1). The polymerizations of **poly(Alk)**, **poly(EG)** and **poly(EEG)** were performed via the previously reported methods (1 mol% Grubbs 2nd generation catalyst, 0.7 M DCM, R.T. for 4 h).(28) **Poly(Urea)** and **poly(Sy)** were prepared in THF at 60 °C due to low conversion at R.T. in DCM. **Poly(Thio)** and **poly(TZ)** also required elevated temperatures, in addition to a higher catalyst loading (2.5 mol% and 5 mol%, respectively). All polymerizations resulted in molecular weights below the theoretical molecular weights based on catalyst loadings, and **poly(TZ)** gave molecular weights below our targeted range (>20 kDa) even at higher catalyst loadings, where the highest molecular weight of **poly(TZ)** obtained was 10.2 kDa.

The inability of the triazole-containing monomer to form high molecular weight polymer is likely due to complexation of the triazole to the Ru catalyst. As previously reported by Kuhn et al., triazole functional groups have been used as ligands in Ru compounds,(40) and triazole-containing monomers have been reported to give low molecular weights under ROMP conditions.(41) The Lewis basic thioether linker may similarly bind to the Ru metal center, inhibiting the polymerization. The fact that Ru metal is retained after reprecipitation at a higher level in these two polymers relative to the other five polymers supports this hypothesis. As measured using inductively-coupled plasma – optical emission spectroscopy (ICP-OES), the **poly(TZ)** and **poly(Thio)** samples exhibited an increase in Ru concentration of 40% and 10%, respectively, after precipitation (Figure S9). For all other linkers, ruthenium concentration remained unchanged or decreased in the precipitated polymer samples. While we have not studied the mechanism of coordination-based disruption in detail, it plausibly involves a combination of intramolecular and intermolecular chelation of functional groups from polymer chains and unreacted monomer to the active site of the catalyst.

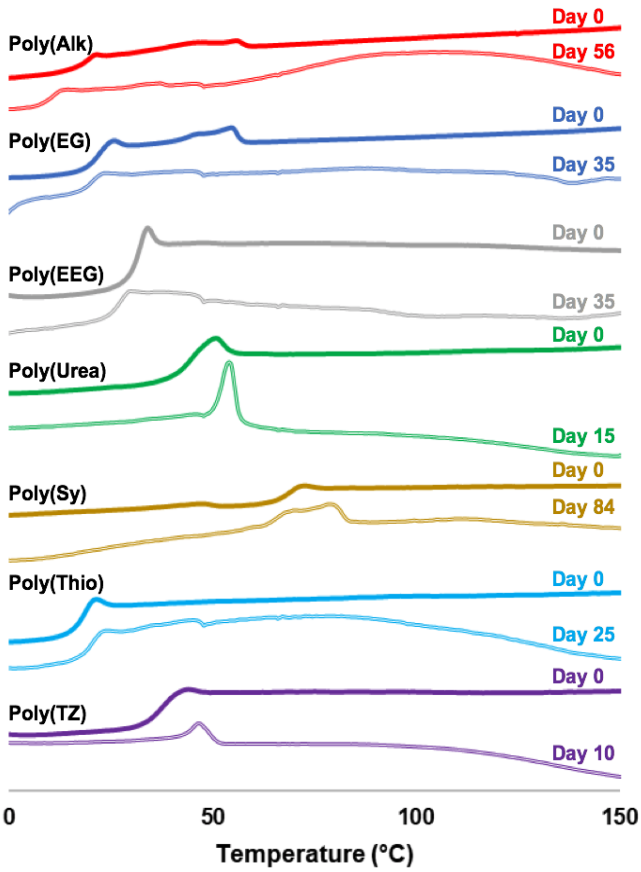

Figure 2. Differential scanning calorimetry thermograms (endo up) of virgin and degraded polymers.

Thermal Properties

Differential scanning calorimetry (DSC) did not show sharp crystalline transitions for the seven polymers, although **poly(Alk)** and **poly(EG)** display broad thermal transitions between 20 – 60 °C that may correlate to the melting of disperse crystalline domains (Figure 2). Neither annealing nor slower cooling rates sharpened these transitions. Similar broad features are seen in the partly degraded samples of **poly(Alk), poly(EG), poly(EEG), poly(Sy)** and **poly(Thio)**.

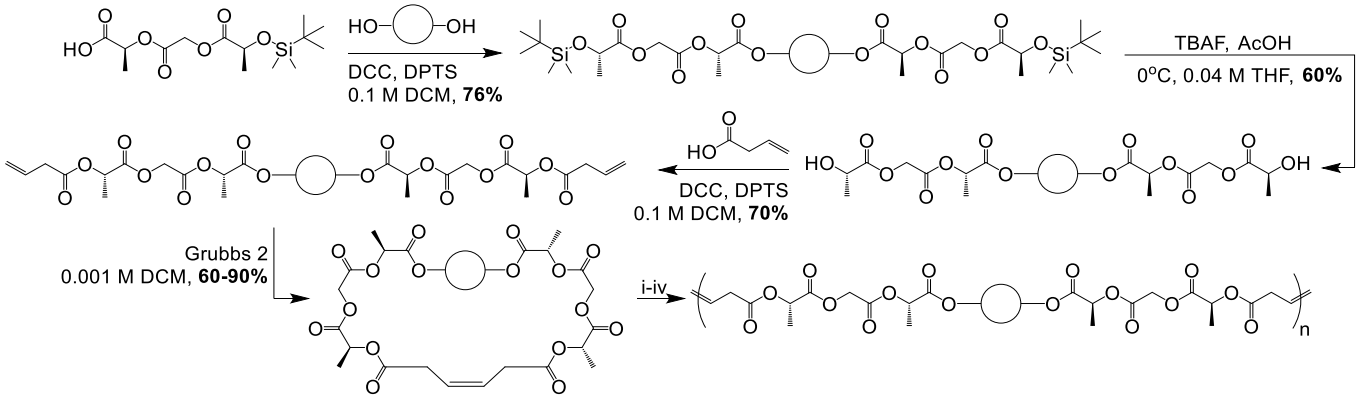

Scheme 1. Example synthetic scheme for the variable linker containing polymers. i (**Alk**, **EG**, **EEG**) – 1 mol% Grubbs 2, R.T., 0.7 M DCM, 4 h, 75%. ii (**Urea**, **Sy**) – 1 mol% Grubbs 2, 60 °C, 0.7 M THF, 4 h, 60-80%. iii (**Thio**) – 2.5 mol% Grubbs 2, 60 °C, 0.7 M THF, 4 h, 76%. iv (**TZ**) – 5 mol% Grubbs 2, 60 °C, 0.7 M THF, 4 h, 68%.

Table 1. Polymer GPC characterization, thermal properties and mechanical properties.

Polymer	M_n[a] kDa	Đ[a]	Predicted T_g[b] °C	T_g[c] °C	T_d[d] °C	E (S.D.)[e] MPa	E_r (S.D.)[e] MPa	S (S.D.)[e] μN/nm	H (S.D.)[e] MPa	P_{MAX} (S.D.)[e] μN
Alk	32.0	1.49	28	19	275	7.2 (0.6)	7.9 (0.6)	0.15 (0.01)	0.47 (0.05)	130 (13)
EG	38.5	1.45	28	21	266	10.0 (0.5)	10.9 (0.6)	0.18 (0.01)	1.5 (0.1)	283 (18)
EEG	30.4	1.46	33	31	267	19.1 (0.3)	21.0 (0.4)	0.39 (0.01)	1.7 (0.02)	416 (6)
Urea	23.1	1.34	41	44	202	19.4 (3.4)	21.3 (3.8)	0.39 (0.07)	1.9 (0.2)	447 (62)
Sy	32.8	1.40	74	68	276	486 (32)	534 (35)	8.1 (0.6)	80 (2)	13,550 (6)
Thio	24.6	1.82	27	18	263	16.3 (1.1)	17.9 (1.2)	0.33 (0.02)	1.4 (0.1)	352 (27)
TZ	10.2[f]	1.54[f]	44	38	240	--[g]	--[g]	--[g]	--[g]	1,040 (200)

[a] Determined by size exclusion relative to polystyrene standards. [b] Determined by the Fox equation, see S.I. [c] Determined by differential scanning calorimetry using second heating cycle at 10 °C/min. [d] Determined by thermogravimetric analysis with heating rate of 10 °C/min. [e] Determined by nanoindentation. [f] Sample not fully soluble. [g] Not reported due to sample-probe adhesion.

The first T_gs of the polymers were predicted using the Fox equation wherein the T_g is estimated by assuming that each component contributes based on its weight fraction and the T_g of the homopolymer with which it is most structurally homologous.(42) In this case, we used the T_g of alternating **Poly LG**(30) reported by Meyer and coworkers for the ester segment, the T_g of polyethylene for the alkene linker region, and the T_g of a polymer with a similar composition to each linker for the variable linker region (poly(ethylene glycol) was used for both the ethylene glycol and thioether linker).(43-45) The weight fractions and T_g values were then used to predict the T_g, which correlated reasonably well with the measured T_g values (Figure S10). Not surprisingly, the T_g was most impacted by moieties that promote interchain interactions, such as the urea and syringic acid linkers. Also, as expected, the weight fraction of the linker segment played a key role.

As for thermal stability, thermogravimetric analysis (TGA) data showed that five of the seven polymers had similar mass loss profiles, with decomposition temperatures (T_d) values in the range of 260-280 °C (Figure S11). The nitrogen-containing polymers, **poly(Urea)** and **poly(TZ)** had slightly lower T_d values of 202°C and 240°C, respectively.

Mechanical Properties

Mechanical data measured by nanoindentation of soft polymer films has its limitations,(46) and the correlation of nanoscale mechanical properties to bulk scale mechanical properties is imperfect. For the purposes of this study however, direct comparison of films via nanoindentation sheds light on the relative mechanical properties of the polymers on a small scale, including hardness (H), stiffness (S), Youngs modulus (E), reduced elastic modulus (E_r) and maximum applied load (P_{Max}).

Mechanical data showed that the linker had a substantial impact on the mechanical properties of the polymer set; **poly(Sy)** has an E of nearly 500 MPa, whereas the other five polymers, excluding **poly(TZ)**, have E's ranging from 7.2 – 19.4 MPa. Hardness values show a large disparity with **poly(Sy)** having a H value of 80 MPa, compared to 0.5 – 1.9 MPa for the other five polymers, again excluding **poly(TZ)**.

As shown by the median load displacement curves in Figure 3, it appears we have prepared three different classes of material. **Poly(Alk), poly(EG), poly(EEG), poly(Thio)** and **poly(Urea)** all seem to be viscous elastomers, **poly(TZ)** showed significant sample-probe adhesion but was a more tough material, and **poly(Sy)** is significantly harder than any of the other polymers.

Sample-probe adhesion is a known source of error in the nanoindentation of soft materials.(46) The load-displacement curves in Figure 3 show that **poly(TZ)** was the only polymer to adhere significantly to the probe, where the adhesion force is proportional to the area of the curve with a negative load value. This adhesion force between the indenter tip and the polymer

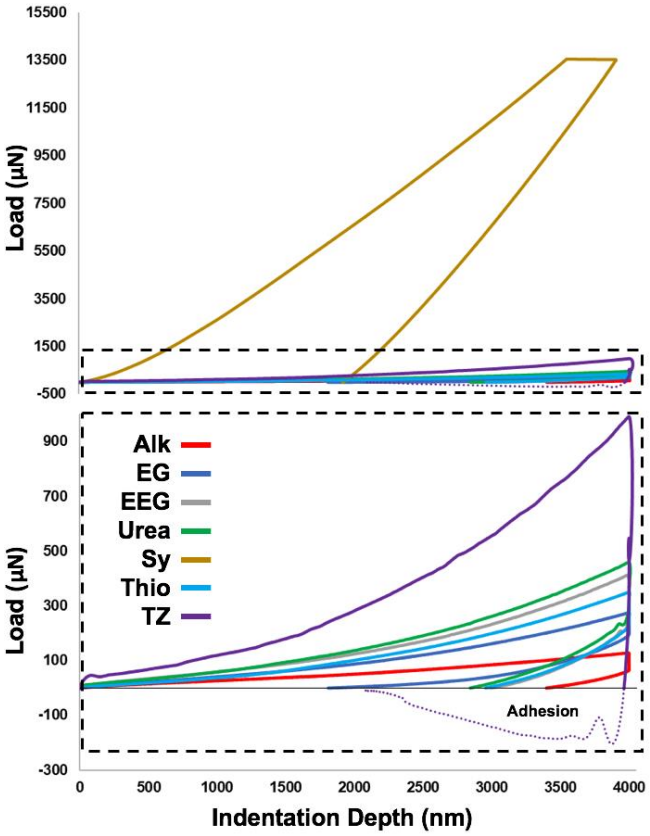

Figure 3. Representative load-displacement curves for each polymer.

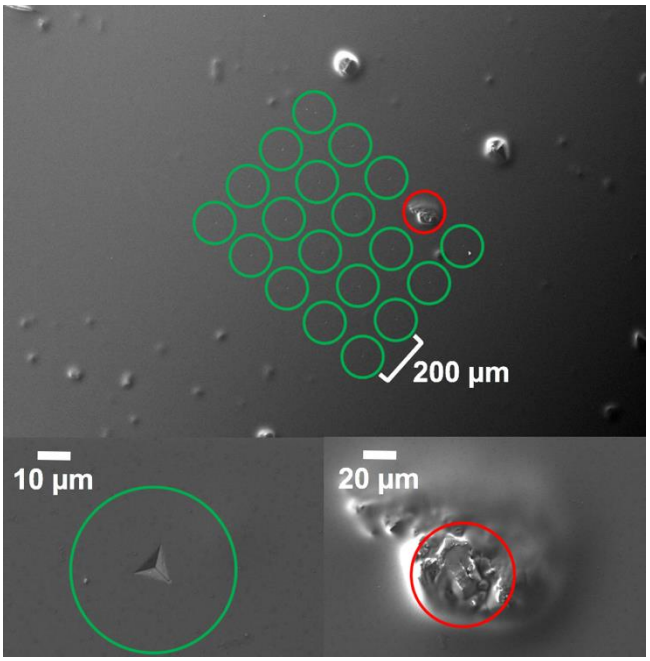

Figure 4. Scanning electron microscopy images of **Poly(Sy)** at 50x (top), 1,000x (bottom right) and 750x (bottom left) (bottom left shows a representative indentation).

sample distorts the calculated H, S, E and E_r. and for this reason, these values are not reported for **poly(TZ)**. P_{Max} should be independent of the sample-probe interactions, and we see that the **poly(TZ)** required over 1,000 µN on average to reach 4,000 nm in depth, more than all but **poly(Sy).** This P_{Max} value is proportional to hardness in all other cases outside of **poly(TZ)**, so we assume that if we were able to optimize indentation to limit adhesion, **poly(TZ)** would be the second hardest of the set, yet still well below **poly(Sy)**.

The indentation sites on five of the seven polymers were imaged using scanning probe microscopy (SPM) (Figure S12). **Poly(Alk)** and **poly(EG)** indentation sites were not located by SPM. As these were the softest of the polymers, it is likely that the indentation sites recovered rapidly. The effect of defects on the measurements could also be directly observed. Scanning electron microscopy (SEM) images of **poly(Sy)** taken after nanoindentation testing showed the grid of 20 indentations (Figure 4). The image shows 19 pyramidal indentations with similar shape and area, and one indentation that was performed on a defect on the surface, which correlates with the only outlier from the **poly(Sy)** indentation dataset, indicating that minor surface defects can lead to drastic outliers, and that the Thompson-Tau method was effective at removing misrepresentative data points.

Film Degradation Study

The hydrolytic degradation of the polymers displayed a large dependence on the linker group. As the degradation of these materials depends on the cleavage of the sequenced ester unit, the magnitude of the influence of the linker groups is somewhat surprising. We hypothesize that the increased hydrophobicity of the syringic acid and alkyl chain containing polymers led to an increased lifespan when subjected to *in vitro* conditions, with

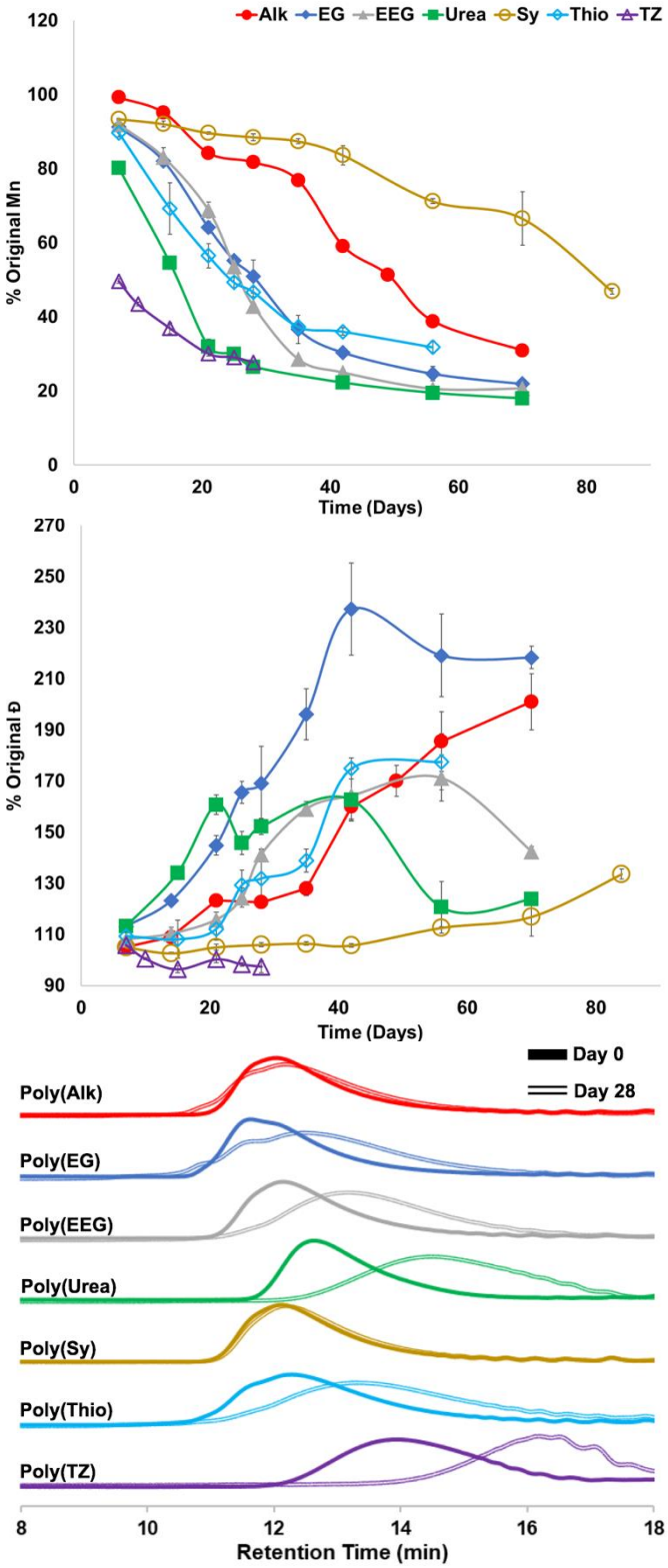

Figure 5. Molecular weight (M_n) (top) and dispersity (middle) as a function of degradation time. Overlay of day 0 and day 28 size exclusion chromatography curves (bottom).

poly(Sy) being the least susceptible to hydrolytic degradation (Figure 5). Consistent with this hypothesis, the replacement of one CH_2 for an oxygen per repeat unit in the **poly(EG)** led to a three-week difference in the time required to reach one half of the polymer's original M_n. Incorporation of a urea functional

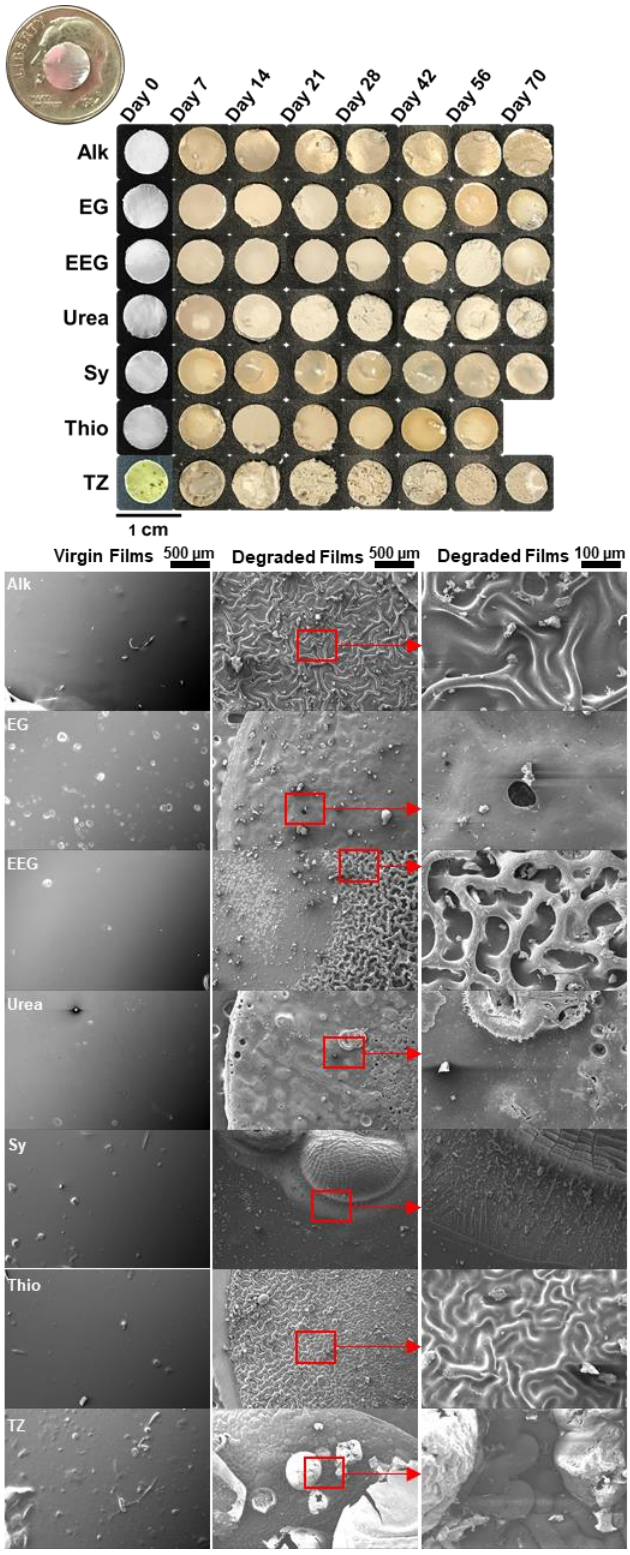

Figure 6. (Top) Pictures of representative polymer films throughout degradation studpy. (Bottom) Scanning electron microscopy images of virgin polymer films at 50x (left), degraded films at 50x (middle) and 250x (right) (location of zoom-in image of degraded **poly(EEG)** is approximate).

group had surprising effects when it came to hydrolytic degradation, as it reached one half of its original M_n the second fastest, behind only the triazole containing polymer. The low solubility of both the virgin **Poly(TZ)** sample and the degraded film samples in THF suggests the molecular weight data obtained via SEC may not be truly representative, yet the early mass loss of the triazole-containing polymer suggests that it is likely the most susceptible to hydrolytic degradation (Figure S13, M_W plot Figure S14, additional GPC data Figure S15). This increased degradation rate is likely due to multiple factors, including a lower virgin M_n, increased hydrophilicity and the presence of a weak organic base, which may catalyze the ester cleavage.

Visually, the polymer films changed from transparent on day 0 to cloudy and opaque as the polymers degrade (Figure 6a). This transition occurs concurrently with loss in molecular weight, as **poly(Urea)** and **poly(TZ)** became opaque far quicker than either **poly(Alk)** or **poly(Sy)**. SEM images show that the surface morphology of the virgin films and degraded films are drastically different (Figure 6b). All seven polymers had similar surface morphology at day 0, yet upon hydrolytic degradation, each seems to have its own unique morphology. Though intriguing, this study did not investigate the causes of these morphological differences, nor attempt to classify the morphologies.

As discussed earlier, DSC thermograms of the degraded polymer films showed a range of different degradation properties (Figure 2). **Poly(Alk)**, **poly(EG)**, **poly(EEG)**, **poly(Sy)** and **poly(Thio)** showed similar thermal transitions to their virgin polymer counterparts, with shifts of few degrees and rougher baselines. **Poly(Urea)** and **poly(TZ)**, both of which have very low molecular weights at the time of observation, show clear melting points and no T_g.

Conclusions

The structure-property relationship of several common linkers and functional groups were tested. We have limited the variables in this study by controlling sequence and molecular weight (excluding **poly(TZ)**), to provide a direct comparison of how the nature of certain moieties affect polymer properties.

Not surprisingly, we discovered in the preparation of these materials that triazole groups and other Lewis bases interfere with ruthenium catalysed metathesis reactions. No optimization was done to prevent such hinderances, but one could presumably provide a more favourable coordination partner, such as copper in the case of a triazole moiety, to limit the interaction of the Lewis base in the monomer/polymer backbone with the ruthenium catalyst.(47)

In our structure-property investigation, we found significant property differences depending on the linker incorporated. Thermal properties were consistent with the linker's ability to promote interchain interactions, i.e., hydrogen bonding with urea units, and pi-stacking with bioaromatics. Mechanical properties were dictated by the linker's rigidity. The rigid bioaromatics in **poly(Sy)** gave mechanical properties orders of magnitude stronger than the rest, followed by **poly(TZ)**, containing a rigid triazole unit. Hydrolytic degradation seemed to be dominated by the relative hydrophobicity of the polymers, as **poly(Sy)** significantly outlasted the rest during *in vitro* hydrolysis. The most staggering example of this phenomenon,

though, was that the exchange of one CH_2 in **poly(Alk)** for an oxygen to give **poly(EG),** nearly halved the lifespan of the polymer.

The data presented suggests that incorporating other functionalities can have large impacts on properties. While it is not surprising that changing the backbone composition of a polymer changes its characteristics, we were surprised at the magnitude of the effect in these systems, particularly the variance in degradation rates as we believed that they would depend primarily on the preserved ester sequence embedded in each monomer. As we discussed in the introduction, linker character is intrinsically important to the SCP field because one primary, scalable route to periodic copolymers is to prepare oligomeric macromonomers and then polymerize them. Moreover, it is common to exploit well-known, high yielding reactions, e.g. click reactions, to assemble the sequenced backbone. Thus, though our study is focused on one-particular class of polymer, we suggest that the results can be extrapolated more generally to any polymerization that creates a periodic SCP separated by structurally dissimilar linkers.

It is important to note that the property changes that are introduced by linkers can also be exploited deliberately. If one understands the impact a linker might have on the properties of a polymer, that understanding can be used to design an optimized material for a targeted application. For example, if one were to desire a degradable material that is tougher than standard PLGAs, but degrades faster, one could incorporate urea/amide linkages, which we have shown strengthens mechanical properties, while promoting degradation.

Conflicts of interest

There are no conflicts to declare.

Acknowledgements

Scott Crawford and Dr. Michelle Ward for their help acquiring and analyzing ICP-OES data.

Notes and references

1. Swisher JH, Nowalk JA, Washington MA, Meyer TY. Properties and Applications of Sequence-Controlled Polymers. In: Lutz J-F, editor. Sequence-Controlled Polymers: Wiley 2017.
2. Laure C, Karamessini D, Milenkovic O, Charles L, Lutz J-F. Coding in 2D: Using Intentional Dispersity to Enhance the Information Capacity of Sequence-Coded Polymer Barcodes. Angewandte Chemie International Edition. 2016;55(36):10722-5.
3. Roy RK, Meszynska A, Laure C, Charles L, Verchin C, Lutz J-F. Design and synthesis of digitally encoded polymers that can be decoded and erased. Nature Communications. 2015;6:7237.
4. Ouahabi AA, Kotera M, Charles L, Lutz J-F. Synthesis of Monodisperse Sequence-Coded Polymers with Chain Lengths above DP100. ACS Macro Letters. 2015;4(10):1077-80.
5. Lutz J-F. Coding Macromolecules: Inputting Information in Polymers Using Monomer-Based Alphabets. Macromolecules. 2015;48(14):4759-67.
6. Al Ouahabi A, Charles L, Lutz J-F. Synthesis of Non-Natural Sequence-Encoded Polymers Using Phosphoramidite Chemistry. Journal of the American Chemical Society. 2015;137(16):5629-35.
7. Trinh TT, Oswald L, Chan-Seng D, Lutz JF. Synthesis of Molecularly Encoded Oligomers Using a Chemoselective " AB plus CD" Iterative Approach. Macromolecular Rapid Communications. 2014;35(2):141-5.
8. Mutlu H, Lutz J-F. Reading Polymers: Sequencing of Natural and Synthetic Macromolecules. Angewandte Chemie International Edition. 2014;53(48):13010-9.
9. Colquhoun H, Lutz J-F. Information-containing macromolecules. Nat Chem. 2014;6(6):455-6.
10. Cole JP, Hanlon AM, Rodriguez KJ, Berda EB. Protein-like structure and activity in synthetic polymers. Journal of Polymer Science Part A: Polymer Chemistry. 2017;55(2):191-206.
11. Altintas O, Artar M, ter Huurne G, Voets IK, Palmans ARA, Barner-Kowollik C, et al. Design and Synthesis of Triblock Copolymers for Creating Complex Secondary Structures by Orthogonal Self-Assembly. Macromolecules. 2015;48(24):8921-32.
12. Edwardson TGW, Carneiro KMM, Serpell CJ, Sleiman HF. An Efficient and Modular Route to Sequence-Defined Polymers Appended to DNA. Angewandte Chemie International Edition. 2014;53(18):4567-71.
13. Hosono N, Gillissen MAJ, Li Y, Sheiko SS, Palmans ARA, Meijer EW. Orthogonal Self-Assembly in Folding Block Copolymers. Journal of the American Chemical Society. 2013;135(1):501-10.
14. van Zoelen W, Zuckermann RN, Segalman RA. Tunable Surface Properties from Sequence-Specific Polypeptoid–Polystyrene Block Copolymer Thin Films. Macromolecules. 2012;45(17):7072-82.
15. Murnen HK, Khokhlov AR, Khalatur PG, Segalman RA, Zuckermann RN. Impact of Hydrophobic Sequence Patterning on the Coil-to-Globule Transition of Protein-like Polymers. Macromolecules. 2012;45(12):5229-36.
16. Schmidt BVKJ, Fechler N, Falkenhagen J, Lutz J-F. Controlled folding of synthetic polymer chains through the formation of positionable covalent bridges. Nat Chem. 2011;3(3):234-8.
17. Soejima T, Satoh K, Kamigaito M. Sequence-regulated vinyl copolymers with acid and base monomer units via atom transfer radical addition and alternating radical copolymerization. Polymer Chemistry. 2016;7(29):4833-41.
18. Zhang S, Bauer NE, Kanal IY, You W, Hutchison GR, Meyer TY. Sequence Effects in Donor–Acceptor Oligomeric Semiconductors Comprising Benzothiadiazole and Phenylenevinylene Monomers. Macromolecules. 2017;50(1):151-61.
19. Norris BN, Zhang S, Campbell CM, Auletta JT, Calvo-Marzal P, Hutchison GR, et al. Sequence Matters: Modulating Electronic and Optical Properties of Conjugated Oligomers via Tailored Sequence. Macromolecules. 2013;46(4):1384-92.
20. Heo H, Kim H, Lee D, Jang S, Ban L, Lim B, et al. Regioregular D1-A-D2-A Terpolymer with Controlled Thieno[3,4-b]thiophene Orientation for High-Efficiency Polymer Solar Cells Processed with Nonhalogenated Solvents. Macromolecules. 2016;49(9):3328-35.
21. Kang TE, Choi J, Cho H-H, Yoon SC, Kim BJ. Donor-Acceptor Random versus Alternating Copolymers for Efficient Polymer Solar Cells: Importance of Optimal Composition in Random Copolymers. Macromolecules (Washington, DC, U S). 2016;49(6):2096-105.
22. Howard JB, Ekiz S, Cuellar De Lucio AJ, Thompson BC. Investigation of Random Copolymer Analogues of a Semi-Random Conjugated Polymer Incorporating Thieno[3,4-b]pyrazine. Macromolecules. 2016;49(17):6360-7.
23. Tsai C-H, Fortney A, Qiu Y, Gil RR, Yaron D, Kowalewski T, et al. Conjugated Polymers with Repeated Sequences of Group 16

Heterocycles Synthesized through Catalyst-Transfer Polycondensation. Journal of the American Chemical Society. 2016;138(21):6798-804.
24. Palermo EF, McNeil AJ. Impact of Copolymer Sequence on Solid-State Properties for Random, Gradient and Block Copolymers containing Thiophene and Selenophene. Macromolecules. 2012;45(15):5948-55.
25. Lutz JF. Sequence-Controlled Polymers: Wiley; 2017.
26. Washington MA, Balmert SC, Fedorchak MV, Little SR, Watkins SC, Meyer TY. Monomer sequence in PLGA microparticles: Effects on acidic microclimates and in vivo inflammatory response. Acta Biomaterialia. 2018;65:259-71.
27. Washington MA, Swiner DJ, Bell KR, Fedorchak MV, Little SR, Meyer TY. The impact of monomer sequence and stereochemistry on the swelling and erosion of biodegradable poly(lactic-co-glycolic acid) matrices. Biomaterials. 2017;117:66-76.
28. Weiss RM, Short AL, Meyer TY. Sequence-Controlled Copolymers Prepared via Entropy-Driven Ring-Opening Metathesis Polymerization. Acs Macro Letters. 2015;4(9):1039-43.
29. Li J, Washington MA, Bell KL, Weiss RM, Rothstein SN, Little SR, et al. Engineering Hydrolytic Degradation Behavior of Poly(lactic-*co*-glycolic acid) through Precise Control of Monomer Sequence. Sequence-Controlled Polymers: Synthesis, Self-Assembly, and Properties. ACS Symposium Series. 1170: American Chemical Society; 2014. p. 271-86.
30. Li J, Rothstein SN, Little SR, Edenborn HM, Meyer TY. The Effect of Monomer Order on the Hydrolysis of Biodegradable Poly(lactic-co-glycolic acid) Repeating Sequence Copolymers. Journal of the American Chemical Society. 2012;134(39):16352-9.
31. Weiss RM, Jones EM, Shafer DE, Stayshich RM, Meyer TY. Synthesis of repeating sequence copolymers of lactic, glycolic, and caprolactic acids. Journal of Polymer Science Part A: Polymer Chemistry. 2011;49(8):1847-55.
32. Misaka H, Kakuchi R, Zhang C, Sakai R, Satoh T, Kakuchi T. Synthesis of Well-Defined Macrocyclic Poly(δ-valerolactone) by "Click Cyclization". Macromolecules. 2009;42(14):5091-6.
33. Yu L, Wang L-H, Hu Z-T, You Y-Z, Wu D-C, Hong C-Y. Sequential Michael addition thiol-ene and radical-mediated thiol-ene reactions in one-pot produced sequence-ordered polymers. Polymer Chemistry. 2015;6(9):1527-32.
34. Besset C, Pascault J-P, Fleury E, Drockenmuller E, Bernard J. Structure−Properties Relationship of Biosourced Stereocontrolled Polytriazoles from Click Chemistry Step Growth Polymerization of Diazide and Dialkyne Dianhydrohexitols. Biomacromolecules. 2010;11(10):2797-803.
35. Macdougall LJ, Truong VX, Dove AP. Efficient In Situ Nucleophilic Thiol-yne Click Chemistry for the Synthesis of Strong Hydrogel Materials with Tunable Properties. ACS Macro Letters. 2017;6(2):93-7.
36. Billiet L, Fournier D, Du Prez F. Step-growth polymerization and 'click' chemistry: The oldest polymers rejuvenated. Polymer. 2009;50(16):3877-86.
37. Gutekunst WR, Hawker CJ. A General Approach to Sequence-Controlled Polymers Using Macrocyclic Ring Opening Metathesis Polymerization. Journal of the American Chemical Society. 2015;137(25):8038-41.
38. Nguyen HTH, Short GN, Qi P, Miller SA. Copolymerization of lactones and bioaromatics via concurrent ring-opening polymerization/polycondensation. Green Chemistry. 2017;19(8):1877-88.
39. Short AL, Fang C, Nowalk JA, Weiss RM, Liu P, Meyer TY. Cis-Selective Metathesis to Enhance the Living Character of Ring-Opening Polymerization: An Approach to Sequenced Copolymers. ACS Macro Letters. 2018;7(7):858-62.
40. Hollering M, Albrecht M, Kühn FE. Bonding and Catalytic Application of Ruthenium N-Heterocyclic Carbene Complexes Featuring Triazole, Triazolylidene, and Imidazolylidene Ligands. Organometallics. 2016;35(17):2980-6.
41. Wei J, Trout W, Simon YC, Granados-Focil S. Ring opening metathesis polymerization of triazole-bearing cyclobutenes: Diblock copolymer synthesis and evaluation of the effect of side group size on polymerization kinetics. Journal of Polymer Science Part A: Polymer Chemistry. 2017;55(11):1929-39.
42. Fox TG. Bulletin of the American Physical Society. 1956;1.
43. Uyama H, Ikeda R, Yaguchi S, Kobayashi S. Enzymatic Polymerization of Natural Phenol Derivatives and Enzymatic Synthesis of Polyesters from Vinyl Esters. Polymers from Renewable Resources. ACS Symposium Series. 764: American Chemical Society; 2001. p. 113-27.
44. Lakouraj M, Hasantabar V, Bagheri N. Synthesis of Polyethers Containing Triazole Units in the Backbone by Click Chemistry in a Tricomponent Reaction2013.
45. Primeaux DJ. Polyurea elastomer technology: history, chemistry & basic formulating techniques. Primeaux Associates LLC. 2004:1-20.
46. Dokukin ME, Sokolov I. On the Measurements of Rigidity Modulus of Soft Materials in Nanoindentation Experiments at Small Depth. Macromolecules. 2012;45(10):4277-88.
47. Schulze B, Schubert US. Beyond click chemistry - supramolecular interactions of 1,2,3-triazoles. Chemical Society Reviews. 2014;43(8):2522-71.

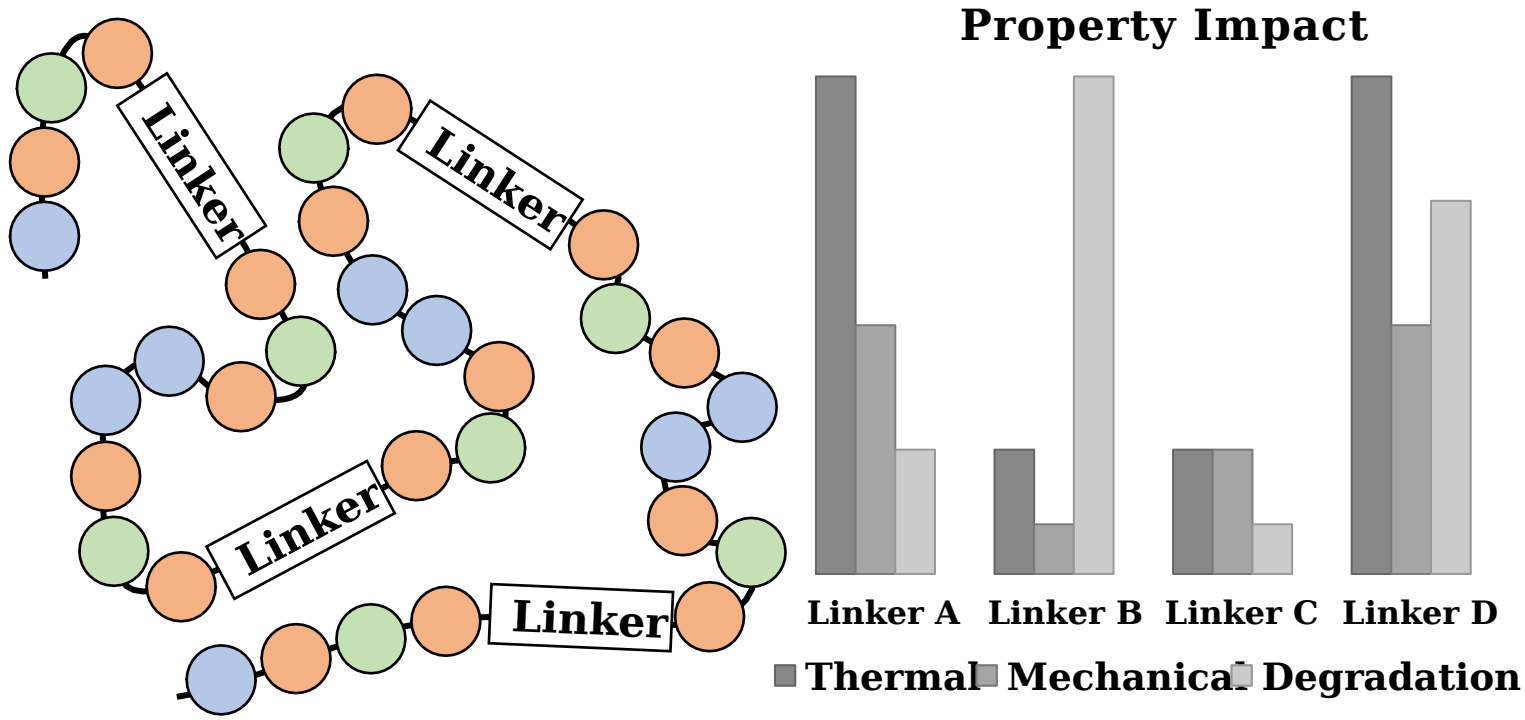

Linker segments in sequence-controlled polyester backbones significantly affect thermal, mechanical and degradation properties.